The Lunar Reconnaissance Orbiter Laser Ranging Investigation

Maria T. Zuber[1], David E. Smith[2], Ronald Zellar[3], Gregory A. Neumann[2], Xiaoli Sun[2], Joseph Connelly[3], Adam Matuszeski[3], Jan F. McGarry[2], Melanie Ott[3], Luis Ramos-Izquierdo[3], David D. Rowlands[2], Thomas Zagwodzki[2], Mark H. Torrence[4]

[1]Department of Earth, Atmospheric and Planetary Sciences, Massachusetts Institute of Technology, Cambridge, MA 02139-4307, USA.
[2]Solar System Exploration Division, NASA Goddard Space Flight Center, Greenbelt, MD 20771, USA.
[3]Advanced Engineering Technology Directorate, NASA Goddard Space Flight Center, Greenbelt, MD 20771, USA.
[4]Stinger Ghaffarian Technologies, Greenbelt, MD 20770, USA.

Submitted to:
Space Science Reviews
Version:
December 20, 2008

Abstract

The objective of the Lunar Reconnaissance Orbiter (LRO) Laser Ranging (LR) system is to enable the spacecraft to achieve its precision orbit determination requirement. The LR will make one-way range measurements via laser pulse time-of-flight from Earth to LRO, and will determine the position of the spacecraft at a sub-meter level with respect to Earth and the center of mass of the Moon. Ranging will occur whenever LRO is visible in the line of sight from participating Earth ground tracking stations. The LR consists of two primary components. The flight system, mounted on the LRO high gain antenna, consists of a receiver telescope that captures the uplinked laser signal, and a fiber optic cable that routes the signal to the Lunar Orbiter Laser Altimeter (LOLA) instrument on LRO. The LOLA instrument receiver electronics record the time of the laser signal based on an ultrastable crystal oscillator, and provide the information to the onboard LRO data system for storage and/or transmittal to the ground through the spacecraft radio frequency link. The LR ground system consists of a pointable laser device at a satellite laser ranging station (NASA's Next Generation Satellite Laser Ranging System, NGSLR) that times and transmits the laser pulse, a data reception and distribution facility, and the LOLA Science Operations Center. Positioning by the LR will enable the determination of a three-dimensional geodetic grid for the Moon based on the precise seleno-location of ground spots from LOLA.

1 Introduction

1.1 Motivation

A primary objective of the Lunar Reconnaissance Orbiter (LRO) mission (Chin *et al.*, 2007) is to perform precise geophysical, geological and geochemical mapping of the Moon to provide an observational framework for future orbital, landed and human exploration. A high-priority component of the mission's exploration objectives is an accurate lunar topography model that will be derived from the Lunar Orbiter Laser Altimeter (LOLA) (Smith *et al.*, 2008a). LOLA's lunar topography model will be used to construct a global, high-accuracy geodetic grid that will provide the foundation for locating data sets from LRO as well as other lunar missions.

1.2 Tracking of LRO

The LOLA instrument has a ranging precision of 10 cm, which is considerably better than orbit determination capability originally baselined for the LRO mission. Uncertainties in spacecraft position thus represent the limiting error source for both the topographic model and geodetic grid. The Moon's synchronous rotation presents a special challenge in determination of the spacecraft orbit because, in the absence of a second orbiter, a spacecraft cannot be tracked directly while orbiting above the lunar far side as viewed from Earth (Lemoine *et al.*, 1997; Konopliv *et al.*, 1998; Konopliv *et al.*, 2001). The spacecraft must be tracked as precisely as possible on the near side so that far side errors do not accumulate above the level that would violate the orbit positioning requirement.

The baseline tracking system for LRO is S-band link for ~20 hours per day. Tracking will be provided by a commercial network, the Universal Space Network, with stations at Dongara, Australia; Kiruna, Sweden; Weilham, Germany; and South Point, Hawaii. The Doppler accuracy of the USN is ~2.5 mm s^{-1}, which for the tracking time allocated will permit LRO orbits to be determined to ~10 m radially and 300 m along-track and across-track.

Altimetric crossovers from the LOLA instrument will also be used in the orbit determination process (Smith *et al.*, 2008a). The use of orbit crossovers has been successfully demonstrated to improve orbits of the Mars Global Surveyor spacecraft (Rowlands *et al.,* 1999) and the gravity field of Mars (Lemoine *et al.,* 2001) using observations from the Mars Orbiter Laser Altimeter (Zuber *et al.*, 1992; Smith *et al.,* 1999; Smith et al., 2001). Simulations of orbit improvement have also been performed for the Vegetation Canopy Lidar (VCL) and ICESat missions (Luthcke *et al.*, 2008). However, the use of crossovers to improve spacecraft orbits has not yet been demonstrated for a spacecraft orbiting a body in synchronous rotation.

An objective of the LRO mission is to determine the radial component of the spacecraft orbit at the sub-meter-level in order to take advantage of the 10-cm range resolution of LOLA and the 50-cm pixel resolution of the Lunar Reconnaissance Orbiter Camera (LROC) (Robinson *et al.*, 2008). These objectives dictated the need for higher-precision tracking on the lunar near side than could be provided with the spacecraft's baselined S-band tracking system and altimetric crossover analysis. Attainment of the precision tracking requirement on LRO will be achieved by introducing a laser ranging (LR) system in which an Earth-based laser will range to LRO whenever in view.

1.3 LR System Overview

As illustrated schematically in Fig. 1, the LR is a one-way time of flight measurement system that uses 532-nm laser pulses to determine the range between an Earth-based satellite laser ranging station and the LRO spacecraft in orbit around the Moon. The system is an innovative combination of proven flight hardware components and satellite laser ranging technology. Stable clock oscillators on the spacecraft and at the Satellite Laser Ranging (SLR) station enable a precise time of flight measurement whenever LRO is in view from the station. The system is designed to measure centimeter-level orbit perturbations over a few seconds of flying time and meter-level perturbations from pole to pole. The LR system has three main elements: the flight segment, the ground station and the data processing system. Tables 1 and 2 list key parameter values for the flight system and ground system elements.

As illustrated schematically in Fig. 2, the LR flight element includes a laser ranging telescope (LRT) attached to the LRO high-gain antenna (HGA), a detector and timing electronics on the LOLA instrument to time-stamp the pulse arrival times, and a fiber optic bundle to transmit the pulses from the LRT to the LOLA detector.

LOLA's Channel 1 detector assembly is designed to receive the LR signal through wavelength division multiplexing, with the LR pulses at 532 nm and the lunar surface returns at 1064 nm. The LR time stamp precision from the LOLA instrument is about 0.5 ns in standard deviation and depends on the signal pulse energy and pulse width.

There are two separate range windows within the LOLA timing electronics, one for the Earth-based laser pulses, referred as the Earth window, and one for the lunar surface returns, referred to as the lunar window. The windows are separated in time to prevent LR measurements from interfering with the lunar surface measurements. The Earth window is 8-ms wide and opens 28 times per second. This window is synchronized with the spacecraft time, which is based on an OCXO stable to $1x10^{-12}$ over an hour period and less than $2x10^{-11}$ per day. The LR range window time can be predicted to <<1ms with respect to coordinated universal time (UTC) after the initial acquisition allowing ground stations to synchronize their pulse arrival to the Earth window.

The LR ground element consists of SLR stations that track the LRO spacecraft as it orbits the Moon and synchronously transmits laser pulses to the spacecraft. The primary ground station for the LR system is NASA's Next Generation Satellite Laser Ranging station (NGSLR), located at Goddard Space Flight Center in Greenbelt, Maryland, shown in Fig. 3. In addition, stations from the International Laser Ranging Service (ILRS) have been invited to partner with the NGSLR facility and participate in ranging activities. While the single NGSLR station is sufficient to meet the LR objectives, the participation from the ILRS will broaden ranging coverage and improve the overall LRO tracking coverage and thus data products.

The NGSLR facility delivers between 1 and 10 fJ of laser energy to the LRO spacecraft. The transmitted laser pulses are 6-ns long and have a wavelength of 532.2 nm. The LR flight system can accept laser pulses up to 15-ns long, but shorter pulses are preferred.

Outgoing laser pulses are time-stamped with < 0.1-ns precision for individual laser shots. The ground-based timing system has a drift rate less than$1x10^{-12}$/hour and an absolute time bias of less than 1 μsec with respect to UTC.

The NGSLR station controls the laser pulse fire times to synchronize the pulse arrival with the LOLA Earth window, compensating for spacecraft movement and Earth rotation.

LR operation is coordinated by the LRO mission operations center (MOC), and the LOLA Science Operations Center (SOC) with the NGSLR facility serving as the single point of contact for ILRS partner stations.

As LR pulses are detected in the Earth window, the LRO spacecraft telemeters confirmation of pulse arrival to the ground in near real time. The data is made available to the ground station to allow for the laser fire time control. The LRO MOC transfers the full set of LOLA science data to the LOLA SOC where the LR pulse transmission and detection times are used to produce ranges to the LRO spacecraft. The 28-Hz data is averaged to produce one range per second valid to ± 10 cm. The ranges are archived in the Planetary Data System (PDS).

The LR is required to achieve LRO's precision orbit determination requirement and will allow the production of a precise geodetic grid from LOLA altimetry (Smith *et al.*, 2008a) that will enable all LRO and many other archived lunar data to be precisely-located on the lunar surface. In addition, the LR range data along with LRO-supplied S-band ranging data and LOLA altimetry data will also be used to generate a refined gravity model of the Moon on a best-effort basis.

2 Flight Segment

Laser signals from the ground station arrive at the LR telescope, shown in Fig. 4, which is attached to the HGA. As illustrated in Fig. 5, the telescope views the Earth through a 3.81-cm diameter, off-centered hole in the primary reflector of the HGA and attaches to the HGA mounting bracket behind the primary reflector.

This location was chosen for the telescope because the HGA will be constantly pointed toward Earth as LRO orbits the Moon and no additional mechanism is necessary to accommodate the LR. The HGA is mounted on two, orthogonal gimbals each capable of rotating 180^{o}, giving the HGA and LRT a hemispherical range of motion. The gimbals' axes are oriented parallel to the Y and X spacecraft axes. Fig. 5 illustrates how the gimbals are attached to the end of a deployable boom mounted to the –Z side of the LRO spacecraft.

LRO will utilize the HGA Ka-band transceiver to downlink telemetry by pointing the HGA at the White Sands Missile Range whenever it is in view. As seen from LRO, the orientation of the Greenbelt Ground Station with respect to White Sands will change depending on the orientation of the spacecraft, the position of the HGA gimbals, and the rotation of the Earth. The LRT field of view was designed to cover nearly the entire Earth while centered on White Sands, NM to maximize ranging opportunities without impacting LRO HGA operations.

A fiber optic cable is used to transfer the signal from the LRT to the LOLA channel 1 detector housing. The fiber optic route passes through each gimbal, down the boom, around the deployment hinge and across the spacecraft deck, covering approximately 10 m in length.

2.1 Optical System

LOLA is mounted on the LRO Instrument Module attached to the +Y side of the spacecraft. The LR optical system transfers the ranging signals from the HGA to the LOLA Channel 1 detector. Ranging signals are collected by the LRT and transferred through the FOB to the LOLA instrument Channel 1 aft optic assembly. The aft optic assembly, which is mounted to the detector housing, filters out non-LR wavelengths and focuses the LR laser pulse onto the channel 1 detector.

The LRT is a pupil imaging design in order to obtain a non-segmented FOV using a multiple fiber-optic cable to transmit the LRT signal to LOLA (cf. Ramos-Izquierdo *et al.,* 2008). As shown in Fig. 4, The LRT has a 30-mrad (~1.7°) field of view with a 19-mm clear aperture, and consists of a sapphire objective lens, a 45° angle of incidence dielectric fold mirror with maximum reflectivity at 532 nm, a 30-mrad (2.74-mm) diameter field stop, and a molded aspheric field lens. A baffle tube assembly limits the optical acceptance angle of the LRT.

The LR-FOB (cf. Fig. 2) is a bundle of seven individual 400 um diameter, 0.22 NA step index fibers. The LR-FOB has three segments. Each segment is terminated at both ends with a common connector assembly that attaches directly to the LRT, the inter-segment couplers and the LOLA aft optic. The connector uses a ferrule to position the fiber end faces in a hex-pattern 1.28-mm in diameter. At the LRT, the ferrule holds the fiber end faces in the plane of focus of the telescope. In the inter-segment connectors, the ferrule ends from two segments abut one another and align the fiber optic end faces of one segment with the fiber optic end faces in the other segment.

The LOLA aft optic assembly re-images the light from the LR FOB into a 600 um diameter image at the surface of the LOLA channel 1 detector. The aft optic includes a 532-nm bandpass filter with 0.3-nm FWHM. The lunar return signal from the LOLA instrument uses the same detector and electronics as the LR signal, but passes through a separate bandpass filter for the 1064-nm signal.

2.2 Mechanical System

The LR telescope is mounted behind the HGA (cf. Fig. 5) and boresignted to it to within 0.01^{o}. The titanium mounting bracket for the antenna is extended away from the gimbal interface. The HGA beam has a divergence of 0.9^{o} and the pointing stability is 0.1^{o} RMS. The telescope looks through a 3.81-cm diameter hole in the HGA primary reflector surface. The telescope upper baffle is partially contained within the conical support structure of the HGA dish. Thermal blanket closeouts are carefully located around these surfaces to prevent solar entrapment while minimizing the risk of accidentally covering the telescope lens.

The LRT lenses are preloaded into an all titanium telescope body. Each convex surface is contacted with a conical mating piece. The field lens, field stop and fiber optic connector receptacle use shims to obtain proper optical distances with respect to each other and to the objective lens. The entire aft field assembly, comprising the field stop, field lens, and fiber optic connector, translates ± 2 mm for optical alignment of the LRT boresight. After alignment, the assembly is liquid-pinned to secure its position.

The LRT fold mirror is mounted using a titanium retainer. But because of a significant mismatch in the coefficient of thermal expansion between the BK-7 mirror and the Titanium retainer, an additional aluminum ring is used between the optic and the retainer to compensate for the mismatch in contraction.

The LRT also has a 340-Ω strip heater bonded to the telescope barrel and wired in series with two thermostats mounted on the aft end of the telescope. Three layers of five mil Aluminum tape are applied over the strip heater to properly distribute heat along the length of the ttelescope. In addition, a NS43C white painted radiator is bolted onto the baffle-telescope interface near the objective lens. The radiator is a half-cylinder with a 22.58-cm^2 area. The material Nusil CV2946 was added to the interface to increase the thermal conductance.

The first section of fiber optic cable runs from the LRT to a connector mounted between the HGA gimbals. To accommodate the full 180^o range of motion for each gimbal without stressing or binding the fiber optic, the cable is routed through the core of the gimbal and spiral wrapped in a thin housing or "slice" attached in a plane perpendicular to the gimbal core. As the gimbal rotates, the spiral cable flexes like a watch spring distributing the tension over the length of the cable in the slice. The second section of fiber optic traverses the Y-axis gimbal in the same way as the first section and runs down the HGA boom under a conduit that provides thermal and radiation protection. After emerging from the conduit, the fiber cable passes around the HGA boom deployment hinge mandrel and attaches to a connector at the base of the -Z panel. The third sections runs along the –Z panel toward the +X panel, then turns and crosses to the +Y panel and goes under the Instrument Module structure where it connects to LOLA.

In areas where the fiber cable could not receive active thermal control and especially at the connectors, the fiber cable is encased in a section of silver-coated copper braided tubing. The ends of the braids are bolted to the aluminum structure to provide passive heating.

Mechanical tie-downs are used to attach the fiber cable to the orbiter. The tie-downs are designed to secure the cable while allowing the fiber to slip along its length, thereby accommodating thermal expansion and contraction. In places, the tie-downs are mounted on stand-off brackets where the cable could not be positioned next to a structure. "S"-bends and loops in the fiber cable route were added during installation to accommodate excess cable length.

3 The NGSLR Ground Station

3.1 Introduction / Overview

The primary ground station for LRO laser ranging is NASA's NGSLR station. NGSLR is the prototype for NASA's next generation of eye-safe, automated SLR stations. NASA's current SLR Network provides two-way ranging to earth orbiting satellites that are equipped with retro-reflector arrays. The laser pulse from the station is time-tagged at pulse emission, travels to the satellite, is reflected off of the array, and is detected and time-tagged by the station's receiver. Approximately 30 satellites are currently being ranged by NASA's SLR stations with altitudes from 500 km to 36,000 km (Degnan, 1993).

NASA is part of the ILRS. (ILRS, 2008; Pearlman *et al.*, 2008). Several ILRS stations will also be participating in LRO-LR as ground stations. The addition of ILRS stations provides global coverage for LR and increases the laser ranging data set.

3.2 NGSLR description

The NGSLR was designed as a prototype to replace the current NASA stations with a more automated, less hazardous, easier to maintain system (McGarry and Zagwodzki, 2006). Operational capabilities of NGSLR include the traditional two-way laser ranging to retro-reflector equipped satellites, and also the ability to perform one-way and two-way transponder laser ranging. During the LRO mission the NGSLR will be used to track the spacecraft when possible and will track Earth satellites at other times. Satellite tracking observations will periodically be used to verify the ground system's pointing.

NGSLR points its telescope at LRO using ILRS predictions called CPFs (Ricklefs, 2006), which are Earth-centered, Earth-rotating vectors spaced at intervals depending upon the orbit. The software interpolates and translates these vectors to the site location and transforms them to the local azimuth and elevation required to drive the mount. The local mount angles are corrected for refraction and mount pointing errors. A Paroscientific model MET3 measures barometric pressure, temperature and humidity, that are used in the calculation of the elevation and range refraction. The mount pointing errors are determined by pointing to stars.

For two-way satellite ranging, the 120-μJ eye-safe laser fires nominally at 2 kHz. A start diode (Motorola MRD 510) picks up the fire events, which are then measured in the Honeywell Event Timer, having a resolution of a few picoseconds and an absolute accuracy of approximately 30 picoseconds. The only control of the 2-kHz laser fire is to set its Pulse Repetition Frequency, not the actual fire time.

Because it must also time tag its laser pulse emission time to much better than 0.2 ns, th NGSLR utilizes a clock oscillator that is stable to a few ns over a 1-hour period. The station time is tied to UTC via the TrueTime (XL-DC) GPS steered Rubidium which provides time to within 100 nanoseconds of UTC. The TrueTime provides a 1pps input to the system Event Timer which becomes part of the data stream. A second timing source, Cesium oscillator (Symmetricom model 4310), which is not steered, provides the 10-MHz external input to the Event Timer. The operational software reads the fire and 1-pps times and records this information to disk for post-processing.

3.3 NGSLR Upgrades for LRO

Several modifications to the basic NGSLR design were required to support LRO. A block diagram of NGSLR as configured for LRO operations is given in Fig. 6. These were: (1) the addition of a higher power, 28-Hz laser, (2) installation of an aircraft avoidance radar, with a range of 20 km, in support of the higher power laser, and (3) control of the laser fire time by the software.

The laser, shown in Fig. 7, is a diode-pumped, frequency-doubled Nd:YAG (532 nm) built by Northrop Grumman Space Technology Cutting Edge Optronics (NGST-CEO) of St. Charles, Missouri. The laser pulsewidth is 5.5 ns (FWHM) and pulse energy is nominally 50 mJ per pulse. The laser is mounted on an upper level breadboard above the NGSLR host system and is coupled into the telescope with a removable aperture share mirror. Final laser beam divergence is controlled with an external beam expander mounted on the upper breadboard The removable mirror allows for easy switching back and forth between NGSLR operations and LRO tracking and permits SLR tracking utilizing the LRO laser for system check out and verification. In testing, the LOLA LR filter was tilt-tuned to the NGSLR LR laser to optimize its transmission.

The Laser Hazard Reduction System (LHRS) provides a means of detecting aircraft before they intersect the transmitted laser beam out to a range greater than the nominal ocular hazard distance. This is accomplished by the use of a pedestal-mounted radar that is slaved and bore-sighted to the laser-transmitting telescope. Upon detection of an aircraft by the radar the LHRS provides a signal to activate a laser beam block. The X-band radar is based on a commercial marine radar that is interfaced with several redundant safety systems that constantly monitor system parameters to ensure proper radar operation and pointing along the laser beam axis.

The NGSLR ground laser fire time is controlled by the station software via the Honeywell Range Gate Generator (RGG) so that each laser pulse arrives at LRO when the LOLA 8-ms Earth Window is open. This allows the Earth pulses to be detected and prevents the pulses from being viewed as background noise by LOLA. The opening of the LOLA Earth Window is synchronized to the spacecraft to 1pps in Mission Elapsed Time (MET). The ground station's time system is UTC. The relationship between UTC and MET is determined by the LRO spacecraft team and is distributed to the LOLA SOC in the form of a piecewise continuous linear function between MET and UTC in a file called the SCLK file. The ground station uses the predictions to calculate the range to LRO and adds this to the anticipated fire time to create the LRO event time. This event time is converted to MET using the SCLK information. If the event falls within the Earth Window the laser is fired, and if not, the software waits for 500 μs before performing the next check.

3.4 Telescope Pointing and Laser Fire Time Control

The LRO position predictions will be generated by the Goddard Flight Dynamics Facility. These predictions have an accuracy requirement of 4 km. Laser ground stations must be able to open loop point their systems to provide between 1 and 10 fJ per cm^2 of laser energy density on LRO at 532.2 nm, while ensuring less than 0.07 mW of peak power on the LOLA detector. NGSLR will range to LRO with 50 mJ per pulse of laser energy, and a 55 mrad divergence. This will provide ~ 2 fJ cm^{-2} on LRO when the Moon's elevation above the ground station horizon is 30^o. NGSLR's peak power will be less than 0.001 mW.

The absolute accuracy of the laser fire measurement must be within 100 ns of UTC with a laser fire inter-arrival time average measurement error of 200 picoseconds or less over a 10-s period. NGSLR's station timing satisfies both of these requirements with the use of the TrueTime Rb Station Timing, the unsteered Cesium external source, and the Honeywell Event Timer.

3.5 ILRS Participation

A few of the participating ILRS stations are also synchronizing their laser fires to the LOLA Earth Window in a similar manner to NGSLR, while several others are firing asynchronously at 5 or 10 Hz. At 10 Hz only 2 to 4 pulses per second will fall in the LOLA Earth Window. The remaining 6-8 pulses will be treated as noise by LOLA, but these are not enough to cause significant problems with the LOLA threshold.

3.6 Feedback to Ground Stations

Since this is an uplink-only ranging measurement, there is no feedback from the laser return as in normal SLR operations. To provide the stations feedback, we are using LOLA's real-time housekeeping telemetry. LOLA's onboard signal processing provides an indication if the earth pulses are arriving at LRO, and also provides where these pulses are occurring in the Earth Window. The LOLA Earth energy monitor also provides an integrated energy over each Earth Window. This information is posted in graphical form to a password protected website that will provide feedback to all participating stations. The delay between spacecraft event and webpage plot should be less than 30 s. NGSLR will be able to bias its fire-times from this information to: (1) search for the Earth Window if no signal is seen in the LOLA housekeeping telemetry, and/or (2) ensure that its laser pulses are arriving as early as possible in the single-stop Earth Window.

3.7 Operations, Data Flow and Scheduling

LRO is visible to Earth for approximately one hour out of every two when the Moon is above the horizon. Laser ranging can only occur above 20^o elevation due to FAA regulations and radar viewing. After each approximately 1 hour long pass, the fire-times and associated information are written to a file in the ILRS CRD format Ricklefs, 2006) which is ultimately transmitted to the CDDIS computer (Noll *et al.*, 2006), where it is picked up by the LOLA SOC for analysis.

The global network of participating stations will be scheduled from a central facility. Laser stations will be scheduled to range during periods that nearby S-band stations have been scheduled for downlink. This will ensure that the real-time feedback to the stations can occur. Initially only one station will be scheduled to range to LRO at a time, however, as the mission progresses, we anticipate two or possibly three ground stations ranging at overlapping times.

4 Link Margin

The LR receiver uses the same Silicon avalanche photodiode detector (SiAPD) as LOLA, but at 532-nm wavelength. The detector sensitivity is about 400 photons/pulse at 95% detection probability under sunlit Earth background. The optical transmission from the LR telescope to the detector is about 40%, which gives a minimum detectable signal level of about 0.2 fJ cm^{-2} at the entrance of the LR telescope. The ranging error improves with the signal level. Fig. 7 shows the receiver probability of detection and the root-mean-square (rms) ranging error as a function of input signal level in both cm^{-2} at the entrance of the LR telescope and photons/pulse on the detector. The desired signal level is 1-5 fJ-cm^{-2}, where the ranging error approaches the noise floor of the LOLA receiver timing electronics. The laser pulse width is assumed to be 8 ns at FWHM points. The ranging error generally improves as the laser pulse width gets shorter but is dominated by the receiver electronics to about 20 cm (0.67 ns) from each laser shot. The receiver also measure the pulse energy which can be used to correct any range-walk associated with the pulse amplitude. The mid- to long-term timing accuracy is governed by the on-board ultra-stable OCXO (Symmetricom 9500), which is stable to better than 3 ns peak-to-peak over several hour period after removing a linear frequency draft rate.

Many of the satellite laser ranging stations around the world can deliver the desired signal level at the LRO distance with a modest laser and beam divergence angle. For example, the primary LR ground station at NASA Goddard Space Flight Center uses a commercially available 6-ns pulse-width 50-mJ diode-pumped Nd:YAG laser and a relatively wide beam divergence angle, 55 μrad (11 arcsec).

5 Data Processing

LOLA science data and Earth ranges are collected at the Science Operations Center (SOC) following each high-gain downlink. Transmit times from each participating Earth station are provided in UTC seconds-of-day, in a common Consolidated Ranging Data (CRD) format. LOLA-LR Earth range signals are calibrated to pulse centroid time with corrections for fixed system biases applied into fractions of the Mission Elapsed Time (MET) count in the LOLA telemetry. The LRO timing system (LRO, 2006) provides a Spacecraft Time Correction Factor (STCF) that converts the MET counter to clock count in UTC. This number of seconds is then used to calculate an approximate UTC arrival time for each Earth range. The difference between the Earth transmit times and the spacecraft UTC seconds, times the speed of light, is the nominal one-way range. The STCF provides the common time system for LRO instruments but has only a 3-ms accuracy requirement, so that further processing is required.

The production process consists of matching ground fires with Earth ranges using a predicted one-way time-of-flight. Production requires predictions of the spacecraft ephemeris, the exported lunar ephemerides with respect to Earth, and the current station positions and Earth Orientation Parameters. The light-time-corrected distance between the ground station and LRO, divided by the speed of light, is added to the fire time. LOLA Earth ranges within a ~10-ms window are matched to these predicted times. If the number of matched differences fills a given 200-ns histogram bin to a significant level, the Earth range times in seconds from midnight are merged with the full-rate CRD data. Normal points consisting of 5-second fits to the valid transmit and receive times in their respective time systems, are provided to the Flight Dynamics Facility and archived with the full-rate data in the ILRS data system.

An example of the value of averaging to produce normal points is given in Fig. 9, which shows observations from the Mercury Laser Altimeter (Cavanaugh *et al.,* 2007). In spite of considerable noise background from sunlit Earth (Fig. 8a, black dots), the signal (red dots) in a 200-ns bin, shown at larger scale in Fig. 8b, can be fit to a linear function to produce a normal point, after removing three outliers.

The raw laser ranges consist of pairs of times that will be recorded by separate clocks, and represent only approximate one-way times. The ground station biases and spacecraft clock drift will be solved for in the course of tracking solutions within the GEODYN/Solve orbit determination software system (Pavlis *et al.*, 2001), applying corrections for time delays due to general relativity. The clock drift will be monitored and correlated with variations in temperature and supply voltage from spacecraft housekeeping to further minimize the drift inherent in the OCXO. The temperature and supply voltage to the OCXO will be monitored from ground and their effects will be modeled and calibrated. The long-term frequency draft will also be monitored and modeled. The residual time base uncertainty is expected to be better than $1 x 10^{-12}$/hours after the initial calibration period. A byproduct will be a much more precise clock correction factor for station fire time prediction and altimetry analysis.

6 LRO Orbit Improvement

LR normal points represent a data type in the determination of precision spacecraft orbits using the GEODYN program. The combination of radio tracking combined with orbit crossovers from the LOLA instrument (Smith *et al.,* 2008a) and optical tracking from the LR, will be used in a best effort basis to improve the gravity field of the Moon to contribute towards selenocentric location of LOLA altimetric shots and the production of a global geodetic grid.

Orbit determination for the LRO mission (Chin *et al.,* 2007) for the current lunar gravity field (Konopliv *et al.,* 2001) has been studied via simulations (Smith *et al.,* 2008b; Rowlands *et al.,* 2008). Table 3 summarizes the various contributions, from S-band tracking, LOLA and the LR, to precision orbit determination of LRO on the basis of the analysis by Smith *et al.* (2008b). Unlike the analysis by Smith *et al.*, the analysis by Rowlands et al. (2008) treats the case of multi-beam rather than single beam altimetry, the former of which is better for orbit improvement from crossover analysis than the latter. However, the analysis of Smith et al. incorporates experience from orbit and gravity field improvement in tracking of Mars Global Surveyor and in particular exploits the power of altimetry in these regards. LOLA's five beams and 10-cm ranging precision along with the LR are expected to eventually result in a radial RMS of order 0.5 m, including orbit and instrument errors, and horizontal errors should approach 10 m. Improvements due to the addition of the LR system are thus significant and will greatly improve knowledge of global and polar topography, footprint-scale surface slopes, and surface roughness. More specifically, inclusion of LR ranges into the orbit determination process allows radial orbit knowledge to improve from 10 m to 1 m, and along- and across-track position to improve from 300 m to <50 m. Knowledge of surface slopes improves from about 2^o to 0.3^o. The LR, however, does not contribute notably to knowledge of surface roughness within the footprint (5-m-scale). Radial and spatial improvements of altimetric footprints map directly into the global geodetic grid.

7 LR Archive

Because LRO does not have requirement for gravity field improvement the Project required improved navigation as an archival delivery to the Planetary Data System (PDS). There is no explicit requirement to deliver the various radio tracking data sets, though the matter is currently under discussion.

The LR component uses LOLA as its data interface and the LOLA Science Operations Center as its pipeline, but is not part of the LOLA archive. The LR full-rate and normal point data will be processed and delivered into the ILRS, using CDDIS/ILRS services as its hosts. Any improved lunar gravity fields that result as a byproduct from the optical tracking of LRO, will be archived with other planetary gravity fields in the Geoscience Node of the PDS.

8 Summary

Key objectives in the LRO mission are determination of a precise global topography model and production of a precise geodetic grid that will serve as a reference for LOLA, other LRO data sets, and many other lunar data sets. Orbit determination is the limiting error source in the LOLA instrument's ability to measure lunar topography, and in the determination of the geodetic grid. The Laser Ranging system was added to the LRO spacecraft to enable the mission's precision orbit requirement to be achieved. The LR will allow LRO orbits to be determined at the meter scale radially and 50 m spatially, and will thus permit the global geodetic grid derived from LOLA to be determined at this level. The LR represents the first time that optical ranging will be used to track a planetary spacecraft and will demonstrate the technology to allow more sophisticated applications in future exploration of the planets.

Acknowledgements

The Lunar Reconnaissance Orbiter Laser Ranging investigation is supported by the NASA Exploration Systems Directorate.

References

CDDIS website: http://cddis.nasa.gov/facility.html.

Cavanaugh, J. F., et al.: 2007, The Mercury Laser Altimeter instrument for the MESSENGER mission, *Space Sci. Rev.* **131,** 451-480, doi: 10.1007/s11214-007-9273-4.

Chin, G., *et al.*: 2007, Lunar Reconnaissance Orbiter overview: The instrument suite and mission, *Space Sci. Rev.*

Degnan, J.: 1993, Millimeter accuracy satellite laser ranging: A review, in D. E. S. a. D. L. Turcotte (ed.), *Contributions of Space Geodesy to Geodynamics: Technology* 25, Geodynamics.

ILRS website: http://ilrs.gsfc.nasa.gov.

Konopliv, A. S., *et al,*: 2001, Recent gravity models as a result of the Lunar Prospector mission, *Icarus* **150**, 1-18.

Konopliv, A. S., *et al.*: 1998, Gravity field of the Moon from Lunar Prospector, *Science* **281**, 1476-1480.

Lemoine, F. G., *et al.*: 1997, A 70th degree and order lunar gravity model from Clementine and historical data, *J. Geophys. Res.* **102**, 16,339-16,359.

Lemoine, F. G., *et al.*: 2001, An improved solution of the gravity field of Mars (GMM-2B) from Mars Global Surveyor, *J. Geophys. Res.* **106**, 23,359-23,376.

LRO: 2006, Lunar Reconnaissance Orbiter Project Timing Specification, LRO NGIN 431-SPEC-000212, NASA/Goddard Space Flight Center, Greenbelt, MD, September 8, 2006.

Luthcke, S.B., *et al.*: 2000, Spaceborne laser altimeter pointing bias calibration from range residual analysis, *J. Spacecraft Rockets* **37**, 374-384.

McGarry, J., and Zagwodzki, T.: 2006, SLR2000: The Path towards Completion, *Proc. 15th Int. Workshop on Laser Ranging*, Canberra, Australia.

Noll, C., *et al.*: 2006, Laser ranging archiving and infrastructure support through the ILRS data centers and web site, *15th International Workshop on Laser Ranging*, Canberra, Australia.

Pavlis, D.E., *et al.*: 2001, *GEODYN Operations Manuals,* Raytheon ITTS Contractor Report, Lanham, MD.

Pearlman, M., *et al.*: 2008, The International Laser Ranging Service, *AOGS Advances in Geosciences: Solid Earth*.

Ramos-Izquierdo, L. *et al.*: 2008, Optical system design and integration of the Lunar Orbiter Laser Altimeter, manuscript in preparation.

Ricklefs, R.: 2006, Consolidated Laser Prediction and Data Formats: Supporting New Technology, *Proc. 15th Int. Workshop on Laser Ranging*, Canberra, Australia.

Robinson, M. S., *et al.*: 2008, The Lunar Reconnaissance Orbiter Camera (LROC), *Space Sci. Rev.*

Rowlands, D. D., *et al.*: 1999, The use of laser altimetry in the orbit and attitude determination of Mars Global Surveyor, *Geophys. Res. Lett.* **26,** 1191-1194.

Rowlands, D. D., *et al.*: 2008, A simulation study of mult-beam altimetry for Lunar Reconnaissance Orbiter and other planetary missions, *J. Geodesy,* doi: 10.1007/s00190-008-0285-y.

Smith, D. E., *et al.*: 2008a, The Lunar Orbiter Laser Altimeter (LOLA) investigation on the Lunar Reconnaissance Orbiter (LRO) mission, *Space Sci. Rev.*, submitted.

Smith, D.E., *et al.*: 2008b, Orbit determination of LRO at the Moon, *7th Int. Laser Ranging Service Workshop,* Oct. 13-17, 2008, Poznzn, Poland.

Figure Captions

Fig. 1 Schematic illustrating the geometry of the LR uplink.

Fig. 2 Schematic showing the LR flight system. The Laser Ranging Telescope (LRT) receives the signal from Earth and transmits it to channel 1 of the LOLA receiver via the fiber optic bundle (FOB).

Fig. 3 NASA's Next Generation Satellite Laser Ranging System (NGSLR) at the NASA/Goddard Space Flight Center, Greenbelt, MD.

Fig. 4 Laser Ranging Telescope (LRT) flight unit. (a) Schematic cutaway. (b) Photograph of flight unit. The LRT is attached behind the LRO High Gain Antenna, viewing through a hole in the primary reflector.

Fig. 5 Schematic showing positions of various components involved in laser ranging on the LRO spacecraft.

Fig. 6 LRO block diagram utilizing the NGSLR as the host tracking system.

Fig. 7 Link analysis results for the LR system. The plot displays the probability of detection and associated range error for signal levels expected during the LRO mission.

Fig. 8 *(a)* Triggers recorded by the Mercury Laser Altimeter on May 27, 2005 versus time (bottom axis), with laser ranges from Earth in red. Axes on left show residual times (s) with respect to predicted range. *(b)* Linear fit to residuals in a 200-ns-wide bin, excluding three outliers.

Table 1 LRO LR receiver parameters

Parameter	Unit
Receiver aperture diameter	1.9-cm clear aperture, 3.0-cm outer diameter
Field of view	30 mrad
Optical fiber bundle	400-μrad core diameter, 7 each, 0.22 NA, step index 40% transmission, including fill factor and connector losses
Optical system transmission	27% transmission, including LOLA aft optics
Optical bandwidth	0.3 nm FWHM*
Wavelength	532 nm
Detector (LOLA Ch. 1)	
Quantum efficiency	45%
Avalanche gain	120
Dark current	83 pA
Preamp noise	1.5 $pA/HZ^{1/2}$
Impulse response pulse width	5 ns FWHM
Timing electronics	
Timing resolution	<0.2 ns
Clock stability	$2x10^{-12}$ over 1 hour
Pulse energy monitor	10% single shot
Range gate	8 ms

*FWHM – Full width at half the maximum amplitude

Table 2 NGSLR Ground Station Characteristics

Parameter	**Unit**
Laser pulse energy	50 mJ
Wavelength	532 nm
Pulse width and rate	<10 ns FWHM, 28 Hz, synchronized to MET
Beam divergence (full angle at $1/e^2$ points	55 μrad (11.3 arcsec)
Pointing uncertainty (3s)	10 mrad (2 arcsec)
s/c position prediction uncertainty	10 μrad (2 arcsec)
Laser optics transmission	50%
Transmission through atmosphere	
Minimum elevation	20^o
Atmospheric transmission	70% zenith 35% 20^o elevation

Table 3 Contributions to LRO orbit improvement and implications for LOLA data products

LOLA Data Products	S-band tracking alone	S-band + LOLA	S-band + LOLA + LR
Global topography - Accuracy/ Resolution	R: 10 m; H: ~300 m	R: 10 m; H: ~200 m	R: 1 m; H: 50 m
Polar topography - Accuracy/ Resolution	R: 10 m; H: ~300 m	R: 5 m; H: 200 m	R: 0.1 m; H: 25 m
Surface slopes			
- Accuracy	2^{o}	1.5^{o}	0.3^{o}
- Resolution	300 m	200 m	25 m
Surface roughness			
- Accuracy	35 cm	35 cm	35 cm
- Resolution	~5 m	~5 m	~5 m

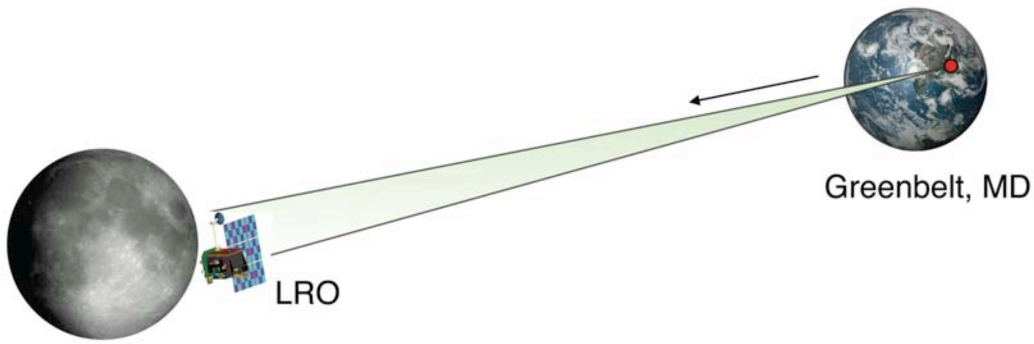

Zuber et al.
Figure 1

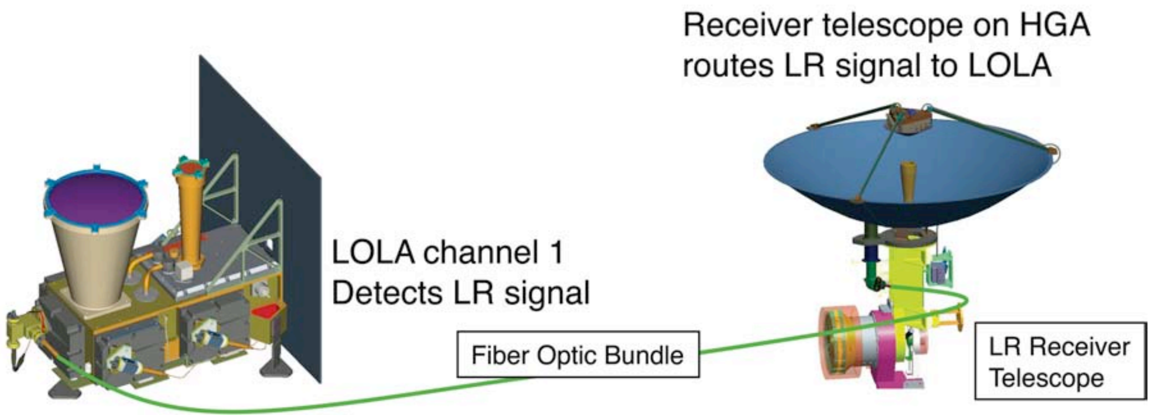

Zuber et al.
Figure 2

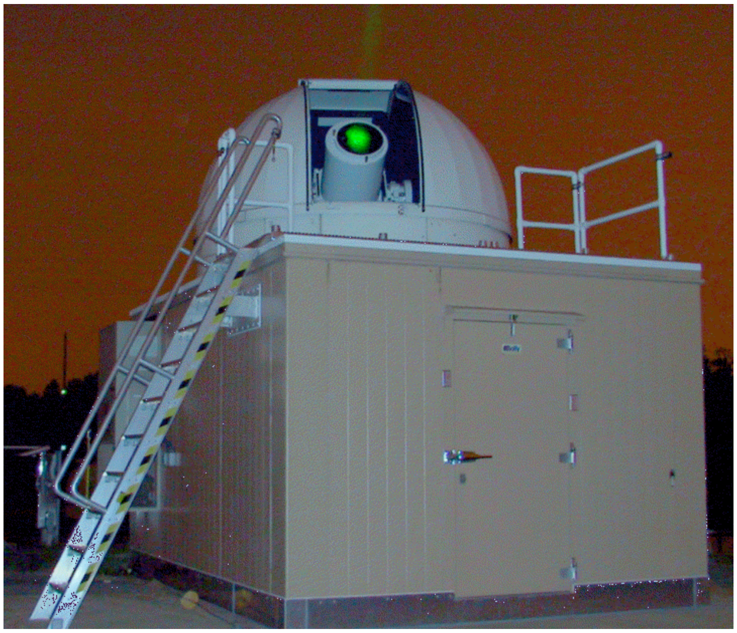

Zuber et al.
Figure 3

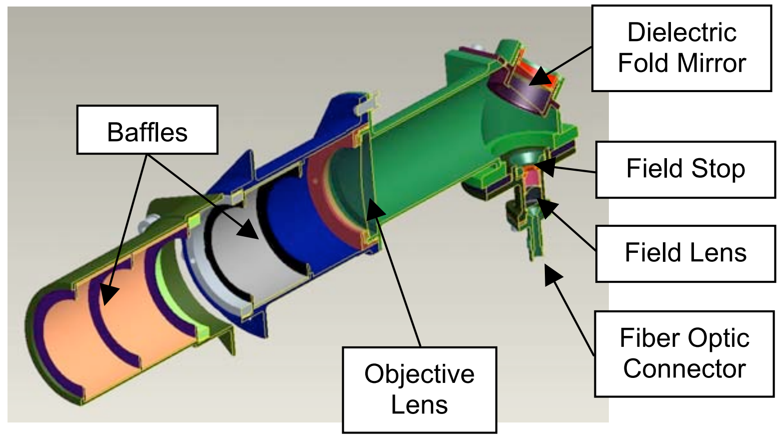

Zuber et al.
Figure 4a

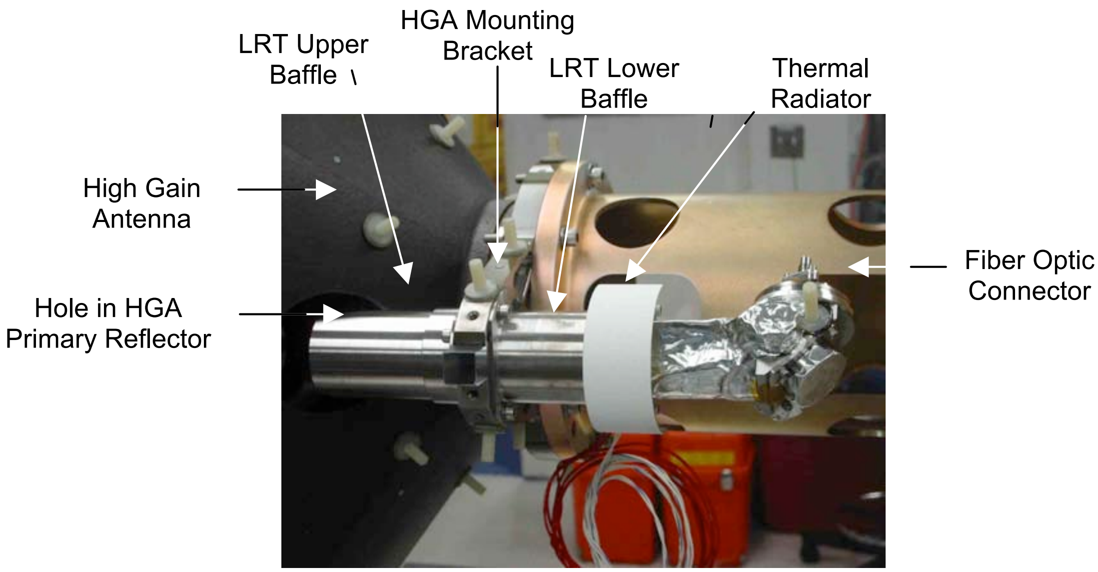

Zuber et al.
Figure 4b

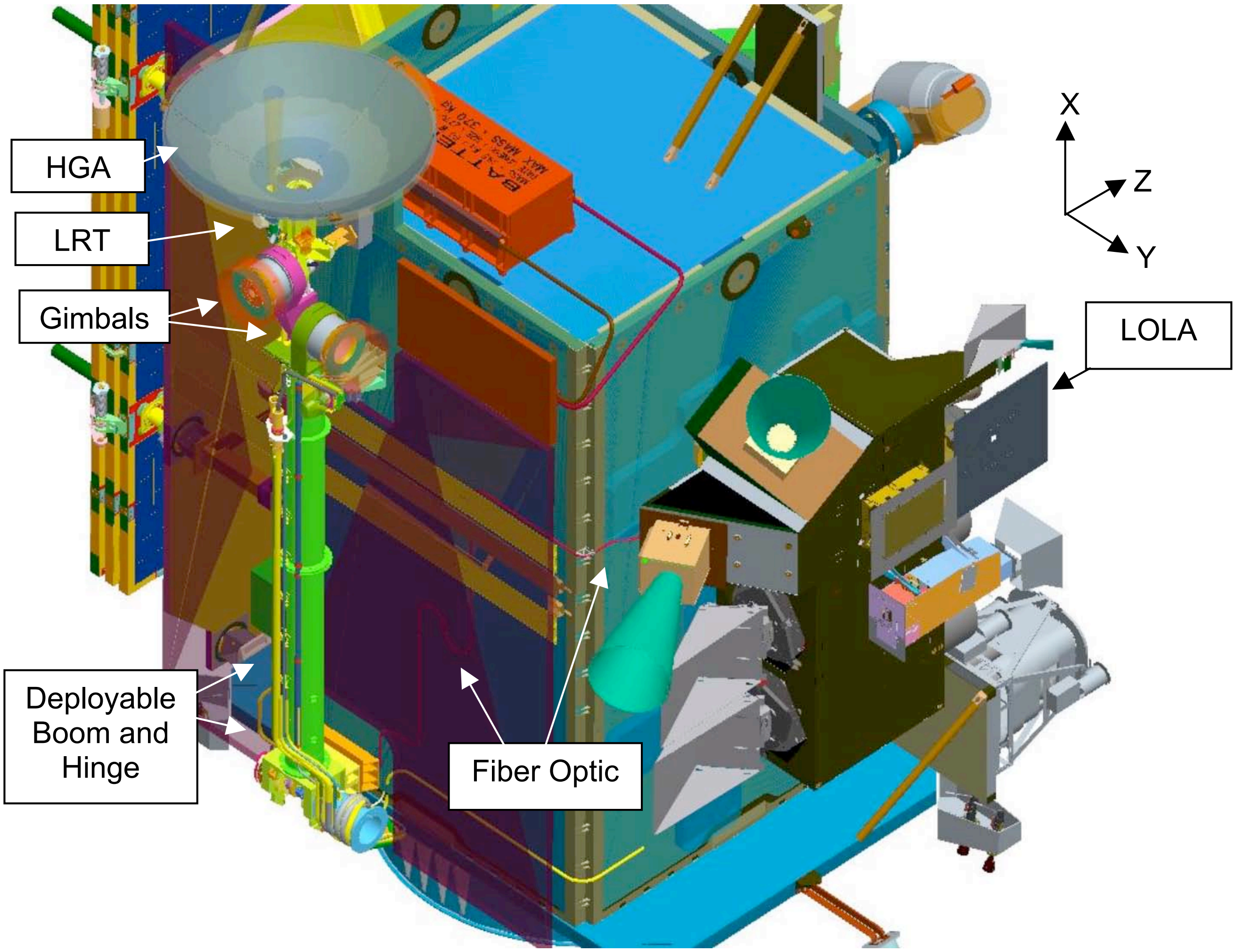

Zuber et al.
Figure 5

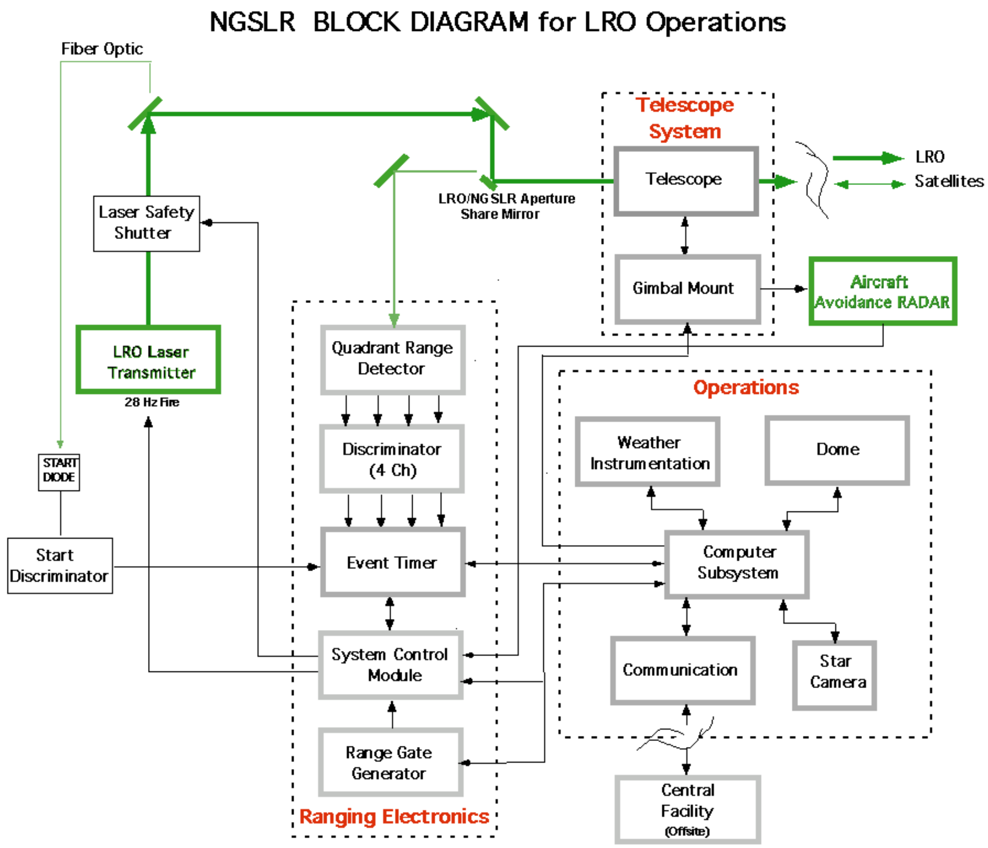

Zuber et al.
Figure 6

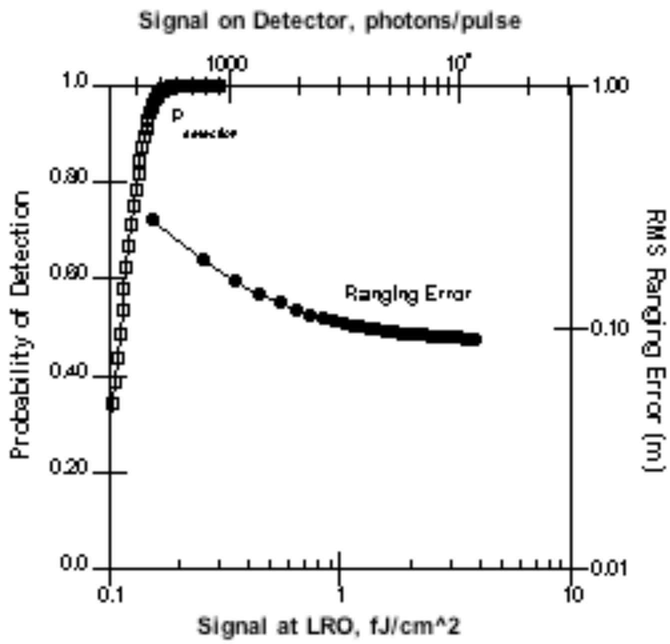

Zuber et al.
Figure 7

a)

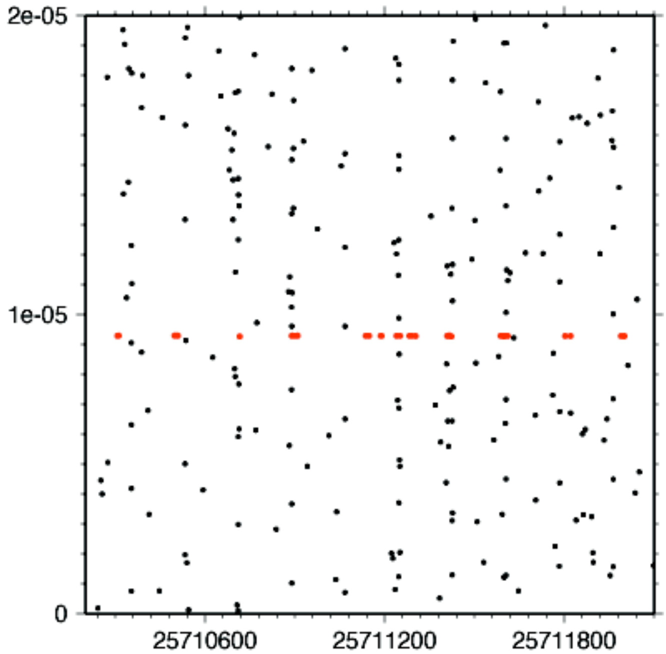

b)

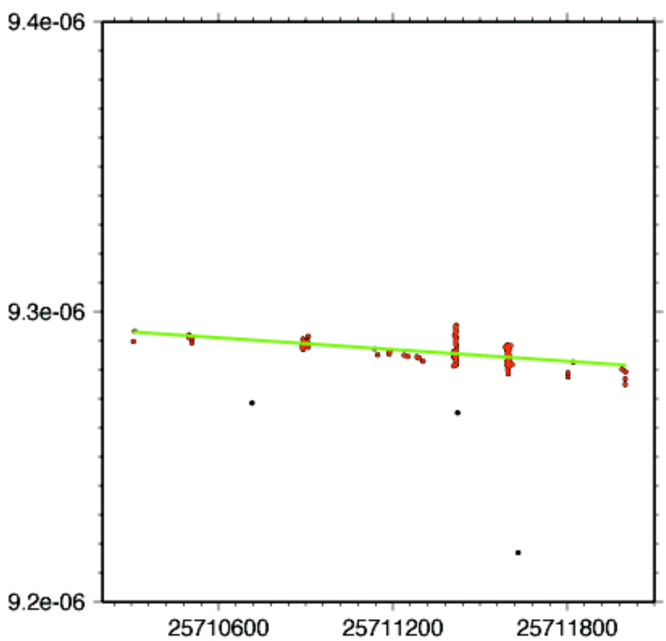

Zuber et al.
Figure 8